$ZnO\text{-}In_2O_3$nanocomposite: An efficient solar photocatalyst

Abinash Das[1], Moumita Patra[1], Manoj Hazarika[1]and Ranjith G. Nair[1, a)]

[1]*Solar Energy Material Research and Testing Laboratory (SMaRT Lab), Department of Physics, National Institute of Technology Silchar, Assam-788010(India)*

a)Corresponding author: rgnair2007@gmail.com

Abstract. Semiconductor photocatalysis is one of the most promising technology to address energy and environmental issues in a self-sustainable manner. Among different semiconductor photocatalysts, Zinc Oxide (ZnO) is one of the most studied photocatalyst. However, the photoactivity of ZnO is limited due to photon absorption in UV range and high charge carrier recombination. Considering the above, the current work report the synthesis of $ZnO\text{-}In_2O_3$ nanocomposite as an efficient photocatalyst through hydrothermal process. The structural, surface, elemental and optical properties of the samples were evaluated using various characterization methods such as X-ray diffraction (XRD), field emission scanning electron microscope (FESEM), energy dispersive X-ray spectroscopy (EDS) and UV-Vis analyses. XRD spectra reveals the high crystallinity of samples with crystallite size distribution in nano range. The FESEM micrographs of the pristine and composite material exhibit nanodisc like structure. An increase in crystallite size is observed for composite material compared to the pristine one and it is in accordance with the XRD results. The absorbance spectra of the composite material shows an elevated redshift towards visible region. Moreover, EDS, XRD and UV-Vis spectra confirms the formation $ZnO\text{-}In_2O_3$ nanocomposite. Photocatalytic performance of the samples were evaluated under solar irradiation using methylene blue as a probe pollutant. The $ZnO\text{-}In_2O_3$ showed superior photocatalytic performance in terms of rate constant and photonic efficiency compared to pristine one. The enhanced photocatalytic performance of the $ZnO\text{-}In_2O_3$ nanocomposite may be attributed to the enhanced photon absorption in visible range and effective charge carrier separation at the composite interface. However more studies are required to confirm the same.

INTRODUCTION

Considering the current environmental demolition and energy crisis, semiconductor photocatalysis has received significant and persistent attention for its ability to address environmental energy issues in self-sustainable manner [1]. In the past several years, a large number of semiconductor materials like metal oxides such as TiO_2, WO_3, ZnO etc. have been reported as photocatalyst [2-4]. It is worth mentioning that among various semiconductor photocatalysts, zinc oxide (ZnO) has been proven to be the most suitable candidate for widespread environmental applications due to its biological and chemical inertness, strong oxidizing power, cost effectiveness, and long-term stability. But ZnO is active only in the ultraviolet region and have moderate photocatalytic performance due to the rapid recombination of photogenerated electron–hole pairs [5]. Among different strategy, using coupled semiconductor can enhance the photocatalytic performance due to the effective electron–hole separation. In recent years, different ZnO based coupled semiconductors ZnO/WO_3, ZnO/TiO_2, ZnO/In_2O_3 have been successfully synthesized for photocatalytic applications. Recently, In_2O_3 has attracted considerable attention as a potential visible light photocatalyst with a band gap of 2.8 eV [6-8]. Thus the coupling of In_2O_3 with ZnO is considered to be an appropriate choice to improve photocatalytic activity in the In_2O_3/ZnO system, in which the role of In_2O_3 is a sensitizer absorbing visible light.

Considering the above, in this study, In_2O_3/ZnO was prepared based on hydrothermal method and consequently the photocatalytic performance of the samples were studied using Methylene Blue (MB) as probe pollutant under solar irradiation. The samples were characterized by X-ray powder diffraction (XRD), field emission scanning

electron microscopy (FESEM), energy-dispersive spectroscopy (EDS) and UV–vis diffuse reflectance spectroscopy (DRS) study.

EXPERIMENTAL

The high purity chemicals such as Zinc (II) nitrate hexahydrate ($Zn(NO_3)_2.6H_2O$), Indium Nitrate hydrate ($In(NO_3)_2.4.5\ H_2O$) , and Sodium hydroxide (NaOH) were used as the precursors without further purification. All the reagents were of analytical grade and Millipore distilled water was used throughout the experiments. For the synthesis of ZnO, $Zn(NO_3)_2.6H_2O$ of appropriate amount was dissolved into 100 ml distilled water and kept in magnetic stirrer at room temperature for 10 minute under vigorous stirring. Then separately prepared NaOH (1M) was added drop wise to the solution at constant stirring to maintain the p^H 10. Then the mixture was transferred in Teflon lined autoclave and heated in an oven at 150^{o}C for 12 hours. After being cooled to room temperature, the obtained solid product was centrifuged, washed three times with DI water and ethanol in order to remove the residues then dried for 12hrs at 150^{o}C. The dried sample were collected and powdered. Finally, the collected samples were calcined at 800^{o}C for 1 hour. The same procedure is repeated for the preparation of ZnO-In2O3 25% (wt %).

CHARACTERIZATION

Structural analyses of the samples were carried out using the X-ray diffraction (XRD) patterns recorded using a diffractometer (Proto Model: AXRD Bench top, Canada). Likewise, surface morphology of the samples were studied by Field Emission Scanning Electron Microscopy (FESEM) images taken using Nova Nano FE-SEM 450 (FEI) operated at 1 kV (TLD-SE) & 1 nm at 15 kV (TLD-SE). The spectral response of the sample was evaluated using a UV- NIR spectrometer with diffuse reflectance attachment (Shimadzu| Model:UV 3600 plus| Origin:Japan).

PHOTOCATALYTIC DEGRADATION EXPERIMENTS

The photocatalytic activity of the samples were investigated under solar irradiation (550 Watt/m2) using methylene blue (MB) as probe pollutant in batch reactor mode. The catalytic material loading of the experiment was kept at 0.5 g/l and the average reactor temperature was maintained at 28^{o}C. The experiments were carried out under solar irradiation for 60 minutes by the simultaneous exposure of the catalysts in 0.01 molar concentration of MB (60 ml) under stirred condition. To ensure adsorption-desorption equilibrium each of the solutions were kept in dark for 2 hrs. The samples were taken from the reactor after every 10 min of exposure using a micropipette. The spectral responses of the centrifuged samples were checked at the wavelength of 664 nm using UV-Visible spectrophotometer (Agilent Technology).

RESULT AND DISCUSSION

Structural analyses of the samples were studied using XRD pattern and shown in Figure 1 (a). The phase composition of the samples were indexed and compared with JCPDS data. All the samples are crystalline in nature and had obvious diffraction peaks corresponding to ZnO and In_2O_3 phases, which indicated that hexagonal ZnO (JCPDS: 750576) and cubic In2O3 (JCPDS: 71-2194) phases were formed. Moreover, the average crystallite sizes of the samples were calculated using the Debye−Scherrer formula [9].

The Field Emission Scanning Electron Microscopy (FE-SEM) images of ZnO and 25 wt. % In2O3 are shown in Figure 1 (c) and (d). The FESEM image of pristine ZnO indicates the formation of randomly distributed nanodisc, whereas in case of composite one, the presence of In_2O_3 along the ZnO clearly shows the modification in the dimensions of the nanodisc structure. Moreover, the energy dispersive X-ray spectroscopy (EDX) and is used to reveal the precise material composition and elemental distribution of nanocomposites (Figure 1 (b)). The EDX mapping of the sample ZnO-In_2O_3 reveals the element distribution of Zn, In and O in ZnO-In_2O_3 nanocomposites. Thus, along with XRD analyses, EDX analyses also confirm the formation of ZnO-In_2O_3 composite.

TABLE 1. Physicochemical Characteristics of the Sample.

Samples	Crystallite Size (nm)	EDS (wt %)			Bandgap (eV)	Rate constant (min^{-1})	Photonic efficiency (%)
		Zn	O	In			
ZnO	18.62		------		3.2	0.05	0.0038
ZnO-In_2O_3	19.47	66.29	15.86	14.93	3.09	0.06	0.0048

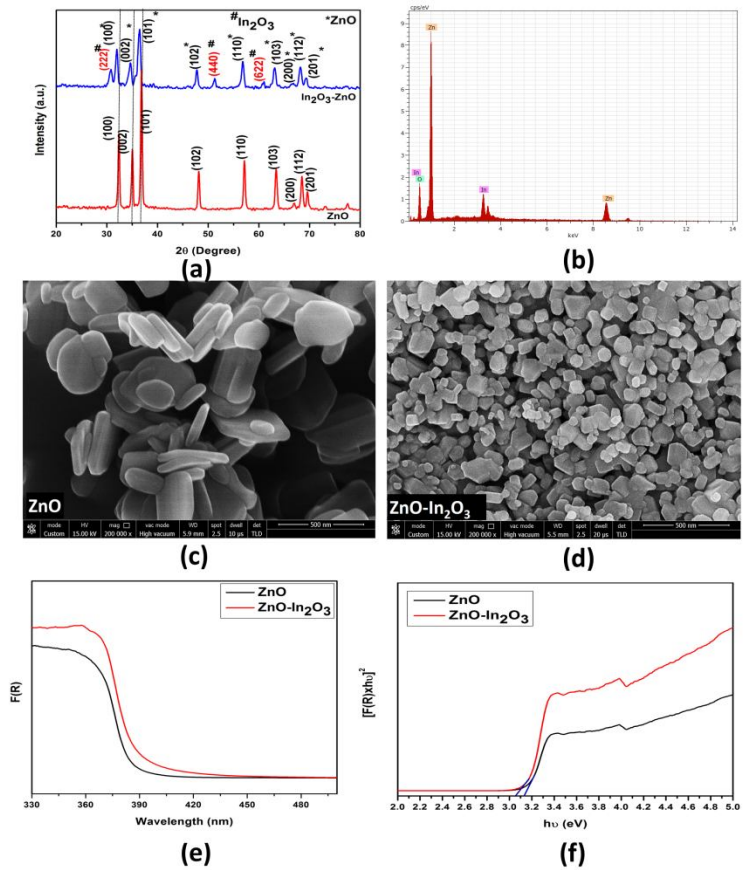

FIGURE 1. XRD spectra (a) EDS image (b) FESEM micrographs of pristine ZnOand ZnO-In_2O_3(c,d) UV-Vis spectra(e) and Tauc's plot (f) of the samples.

Figure. 4 shows the UV–vis absorption spectra of the samples. The pristine ZnOnanodisc shows a strong absorption in the ultraviolet region whereas the composite sample showed the elevated red shift in absorption (Figure 1 (e)). Which can be attributed to the formation of ZnO-In_2O_3 composite. In addition, the band gap of samples were calculated using modified Tauc's relation by plotting [F(R)hυ]2 vs. hυ as shown in Figure. 1(f) and the values are depicted in table 1 [10]. The observed slight red shift in the band gap is due to formation of composite between ZnO and In2O3.

The photocatalytic performance of the samples were studied in batch mode reactor. Methylene Blue (MB) is used as probe pollutant to study the degradation spectra of the sample under solar irradiation. The degradation kinetics of the samples with respect to time is shown in Figure 2 (a). Moreover, the rate constant of the samples was calculated by plotting time and -ln(C/C_o) (Figure 2 (b).) and the values are depicted in Table 1 [11]. As expected from the physicho-chemical analyses of the sample, ZnO-In_2O_3 show better photocatalytic performance than the pristine one. The enhanced photocatalytic performance of the composite sample is mainly governed by the synergic

effect of efficient charge carrier separation due to the heterostructure, visible light harvesting proficiency of In_2O_3, and the formation of preferential adsorption sites on the surface of nanodisc like structure [12].

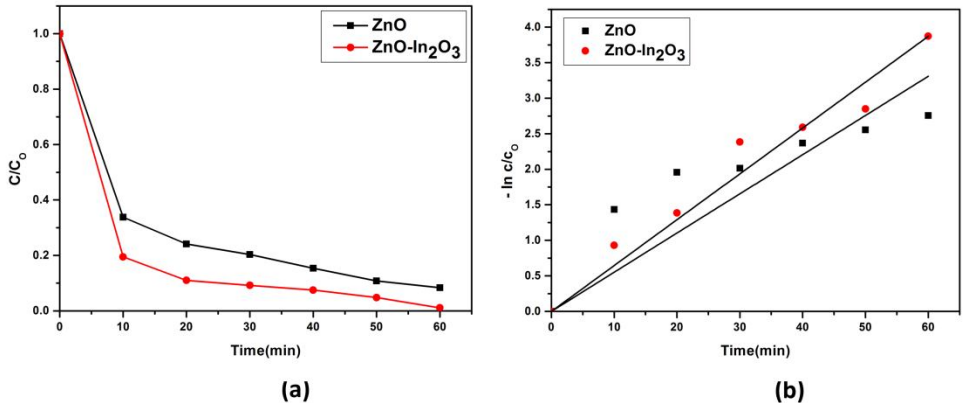

FIGURE 2. MB degradation spectra (a) and rate constant calculation spectra (b) of the samples.

CONCLUSION

In summary, nanodisc like ZnO-In_2O_3 composite is prepared through hydrothermal method for photocatalytic application. The X-ray diffraction (XRD) pattern and energy-dispersive X-ray (EDX) spectrum confirms the presence of In_2O_3 along with ZnO. Moreover, the FESEM micrographs reveals the formation of unique nanodisc like structure contributing more active sites for solar energy utilization. Compared to the pristine ZnO, the enhanced photocatalytic performance of the composite sample can be ascribed to the effective charge carrier separation at their interface and elevated absorption towards visible region.

ACKNOWLEDGMENT

The financial support provided by the Inter University Acceleration Centre, New Delhi vide Project no. UFR-58315 and DST-SERB, New Delhi vide project no. ECR/2016/001186 is gratefully acknowledged.

REFERENCES

1. Liangliang Zhu, Minghui Hang, Ghim Wei Ho, Sci. Rep. **511609**, 1-11 (2015).
2. AnjaluRamchiary, S.K. Samdarshi, T. Shripathi, Sol. Energy Mater Sol. Cells. **155,** 117–127 (2016).
3. Diana B. Hernandez Uresti, D. Sanchez-Martinez, A. Martinez-de la cruze, Ceram Int. **40**, 4767-4775 (2014).
4. Yuting Wang, et al.,Sci. Rep. **632711,** 1-10 (2016).
5. Xinyu Zhang, Jiaqian Qin, YananXue, Pengfei Yu, Bing Zhang, Limin Wang and Riping Liu, Sci. Rep. **44596,** 1-8 (2014).
6. Sze-Mun Lam, Jin-Chung Sin, Ahmad Zuhairi Abdullah, Abdul Rahman Mohamed, J. Colloid Interface Sci. **450**, 34–44 (2015).
7. EylemTopkaya, Mehmet Konyar, H. CengizYatmaz, KorayOzturk, J. Colloid Interface Sci. **430**, 6–11 (2014).
8. Zeyan Wang, Baibiao Huang, Ying Dai, Xiaoyan Qin, Xiaoyang Zhang, Peng Wang, Haixia Liu,Jiaoxian Yu, J. Phys. Chem. C. **113**, 4612-4617 (2009).
9. Abinash Das, P. Malakar, Ranjith G. Nair, Mater. Lett. **219** 76–80 (2018).
10. Simelys Hernández, ValentinaCauda, Diana Hidalgo, Vivian Farías Rivera, Diego Manfredi, Angelica Chiodoni, Fabrizio C. Pirri, J. Alloy. Compd. **615,**530–537 (2014).
11. Ranjith G. Nair, Abinash Das, Samrat Paul, B. Rajbongshi, S.K. Samdarshi, J. Alloy. Compd. **695**, 3511-3516 (2017).
12. Na Wei, Hongzhi Cui, Xinzhen Wang, Xiang Xie, Mingliang Wang, Liqiang Zhang, Jian Tian, J. Colloid Interface Sci. **498**, 263–270 (2017).